Submitted to Nuclear Physics A

LBL-5814
Preprint C.|

SHELL MODEL THEORY FOR PERIPHERAL COLLISIONS

J. P. Boisson, J. G. Ioannou, T. Shibata, and
J. O. Rasmussen

November 1976

Prepared for the U. S. Energy Research and
Development Administration under Contract W-7405-ENG-48

SHELL MODEL THEORY FOR PERIPHERAL COLLISIONS+

J. P. Boisson*, J. G. Ioannou,

T. Shibata**, and J. O. Rasmussen

Lawrence Berkeley Laboratory
University of California
Berkeley, California 94720

ABSTRACT

Relativistic heavy-ion peripheral collisions are treated by introducing a Gaussian time-dependent, surface interacting perturbation model, and results for 250 MeV/N projectiles on ^{88}Sr and ^{32}S are compared with those of previous Monte Carlo calculations as well as experiment.

+This work was done with support from the U.S. Energy Research and Development Administration.

*Present address: IN2P3, Institut des Sciences Nucléaires, B.P. 257 Centre de Tri, 38044 Grenoble-Cedex, France.

**Present address: Physics Department, Osaka University, Toyonaka, Osaka, Japan.

1. Introduction

Monte Carlo calculations[1]) based on the cascade-evaporation model have enjoyed considerable success in explaining reactions of nucleons with nuclei in the 100 MeV - 1 GeV energy region. A related picture, the abrasion-ablation model[2]), has been applied with relative success to the recent data on relativistic heavy ion fragmentation[3]). All these calculations have had some degree of difficulty with the simplest reactions, such as, one-nucleon removal and inelastic scattering to bound excited states, usually underestimating the cross section. Indeed, the abrasion-ablation model calculations[3]) do not include inelastic scattering at all. There are known cases of irregular behavior that are associated with shell structure. Karol and Miller[4]) have studied and explained such anomalies in terms of nuclear skin thickness variations. Benioff[5]), specializing to the energy regime well above 1 GeV, has treated the peripheral reactions by taking into account nuclear surface- and shell-structure effects.

There has, so far as we know, been no attempt to relate these theories to inelastic scattering for which data at energies above 100 MeV have only recently been obtained[6]). The (p,p') data of Bertini *et al*[7]) at 1 GeV on ^{12}C, ^{58}Ni, and ^{208}Pb give considerably larger inelastic scattering cross section to the first excited states alone than the Monte Carlo cascade calculations give. This discrepancy was discussed by Ejiri *et al*[8]) in their paper on relativistic carbon ion peripheral reactions.

2. The Scattering Model

The model we use is most simple in concept. The initial state is a set of protons and neutrons in individual orbitals in a Woods-Saxon potential well. The grazing particle (projectile) is assumed to manifest itself as a time-dependent perturbing potential pulse sharply located in space at the edge of the nucleus (target). The time-dependent Schrödinger equations are integrated from $-\infty$ to $+\infty$ for all particle-hole amplitudes of interest and for excitations of nucleons from particular orbitals to states in the continuum.

In the calculations to be presented here the time dependence is taken as a Gaussian and the spatial dependence as a delta function. However, we shall later discuss correction factors for the spatial delta function approximation.

Our static Hamiltonian is the usual one of the nuclear shell model for non-interacting particles and is given by

$$H_o = \sum_i - \frac{\hbar^2}{2\mu} \Delta_i + V(\bar{r}_i, \bar{\sigma}_i) \tag{1}$$

where in (1) $V(\bar{r}_i, \bar{\sigma}_i)$ is chosen to be the Woods-Saxon potential with form and parameters as given by Soloviev[9]).

Our time-dependent perturbing Hamiltonian term is of the form:

$$H'(r_i\theta_i,\phi_i,t) = \left[V_1 \prod_{1 \leqslant i \leqslant A} \delta(r_i - R_1)\ \delta(\theta_i)\right] \exp\left(-\ (t/t_o)^2\right) \tag{2}$$

where r_i, θ_i, ϕ_i, are coordinates of the target nucleons with respect to the target center, the z-axis being chosen to go through the point of closest approach of the projectile. R_i is a parameter to be chosen near the target radius R_t, and t_o is the characteristic collisions time.

Let us suppose that the target is even-even with closed orbitals. The time-dependent Schrödinger equation for the amplitude of various particle-hole excited states is

$$\dot{\alpha}_{a,b} = -\frac{i}{\hbar} < ab \, |H'| \, 0 > \alpha_o(t) \, \exp\left(\frac{i \, E_{ab} t}{\hbar}\right) \tag{3}$$

where in (3) as well as in what follows a,b stand for the particle, hole states, respectively, and o refers to the initial (ground) state. Also in (3), E_{ab} is the excitation energy of a particle-hole state corresponding to the scattering of a nucleon from a bound orbital of energy E_b to another of energy E_a. Finally, the initial conditions ($t=-\infty$) for eqs. (3) are ground state amplitude $\alpha_o(-\infty) = 1$ and all others $\alpha_{ab}(-\infty) = 0$. If we consider in perturbation theory that $\alpha_o(t)$ remains unity, then the time integral can be analytically carried out. The spatial integral is also very simple with the delta function operator. Thus, we obtain

$$\alpha_{a,b}(\infty) = -\frac{i}{\hbar} \int_{-\infty}^{+\infty} dt \, \exp\left[-\left(\frac{t}{t_o}\right)^2 + i\left(\frac{E_{ab} t}{\hbar}\right)\right] \times$$

$$\delta_{m_a,\pm 1/2} \, \delta_{m_b,\pm 1/2} \frac{V_1}{8\pi} (2J_a+1)^{1/2} (2J_b+1)^{1/2} \mathcal{R}_a(R_1) \, \mathcal{R}_b(R_1) \tag{4}$$

with J_a, J_b the particle, hole spins respectively and $\mathcal{R}_a(R_1)$, $\mathcal{R}_b(R_1)$ the respective radial parts of the wave functions calculated at R_1. We observe in (4) that only states with projections $m = \pm 1/2$ which do not have nodes on the z-axis contribute; the angular part of the matrix elements is simply the product of $(2J+1)^{1/2}$ factors, and the radial matrix element is just a product of radial functions evaluated at a certain distance. Then the transition probability of the particle-hole state excitation (a,b) is

$$P_{a,b} = \frac{(2J_a+1)\ (2J_b+1)}{32\pi} \left\{ \frac{V_1 t_o}{\hbar} \mathscr{R}_a(R_1)\, \mathscr{R}_b\ (R_1)\ \exp\left[-\left(\frac{E_{ab} t_o}{2\hbar} \right)^2 \right] \right\}^2 . \qquad (5)$$

Similarly, the transition probability for the struck nucleon to be excited from a bound state a of spin J_a to a state of the continuum c with the angular momentum I_o, spin J_c and energy E_c is

$$P_{a,c} = \frac{(2J_a+1)(2J_c+1)}{32\pi} \left[\frac{V_1 t_o}{\hbar} \mathscr{R}_a\ (R_1) \mathscr{R}_{L_c,J_c}(R_1,\ E_c) \right.$$

$$\left. \times \exp\left(- \left[\left(\frac{E_{ac}\ t_o}{2\hbar} \right)^2 \right) \right] \right]^2 \qquad (6)$$

In order to obtain the probability for the struck nucleon to be excited from a bound state to any state of the continuum we have to make in (6) a summation over all possible values of L_c, J_c and integration over E_c from 0 to infinity.

At this point we wish to derive a correction factor for the spatial delta function dependence of the perturbing Hamiltonian term of eq. (2). Suppose $\delta(\theta)$ in the perturbing Hamiltonian given by (2) is replaced by a finite range angular factor

$$\exp \; -\left[\theta^2 R_1^2/r_o^2\right]$$

Then, ignoring nuclear spin, we have the matrix element factor

$$A = \int Y^*_{\ell_f 0} \exp\left[-\,\theta^2 R_1^2/r_o^2\right] Y_{\ell_i 0}\, d^3\bar{r}$$

To simplify the calculation of A without loss of generality we can assume that the initial $\ell_i = 0$ since the correction factor contributes more for $\ell_f - \ell_i >> \ell_i$ which is the case for ℓ_i that of a bound state and for ℓ_f that of a state of the continuum. Thus we have

$$A = \int Y^*_{\ell 0} \exp\left[-\,\theta^2 R_1^2/r_o^2\right] Y_{oo} \quad \sin\theta\; d\theta d\phi$$

Replacing the spherical harmonics by their asymptotic Bessel-function expansion and approximating the upper limit of θ integration by ∞ we obtain

$$A = \text{const.} \int_o^\infty J_o \left[(2\ell+1)\,\sin\theta/2\right] e^{-\theta^2 R_1^2/r_o^2} \sin\theta\; d\theta$$

We finally obtain for A, by evaluating the integral, an expression which is proportional to the factor

$$\exp\left[\frac{-(\ell+1/2)^2 r_o^{\,2}}{4\,R_1^2}\right]$$

Hence, we introduce such an angular-momentum transfer correction factor.

Multiplying eq. (6) by

$$e^{-\left(\frac{L_c}{L_o}\right)^2} \tag{7}$$

The corrected eq. (6) can be summed and integrated as before to get knock out probabilities from any given occupied state.

Let us now estimate reasonable values for the parameters V_1, t_o, and L_o. First of all, there is no unambiguous way of determining the absolute strength V_1 of the time-dependent perturbing Hamiltonian of eq. (2). It is related to a radial integral over a nucleon-nucleus optical model potential. For this paper we leave V_1 a paremeter and only study relative cross sections. Next we estimate t_o. One way of estimating it, if the nucleon-nucleon interaction is dominant and the collective field of the nucleus ignored, is to take it equal to r_o/v where r_o is the effective nucleon-nucleon interaction range and v the velocity of the incoming projectile nucleus. Of course, this value for t_o assumes a one nucleon - one nucleon interaction at any time. Another approach to estimate t_o is the one in which we attempt to take into account the size of the target nucleus. In this case, assuming a straight-line trajectory for the projectile - which is reasonable for energies above 100 MeV - , and considering the effective nuclear-nuclear interaction as a Yukawa potential of depth V and range r_o, then for a nucleon trajectory tangent to the target nuclear surface of radius R_t the distance from it goes as follows:

$$s(t) = (R_t^2 + (vt)^2)^{1/2} - R_t \tag{8}$$

If we assume $R_t >> r_o$, eq. (8) can be approximated by

$$s(t) \simeq \frac{1}{2} \frac{(vt)^2}{R_t} \tag{9}$$

The time-dependent interaction, as felt at the nearest point of the surface, is

$$V(t) = - \frac{v}{s(t)} \exp\left(- \frac{s(t)}{r_o}\right) \tag{10}$$

Introduction of eq. (9) into eq.(10) yields for V(t)

$$V(t) \simeq \frac{2vR_t}{(vt)^2} \exp\left[- \frac{(vt)^2}{2r_o R_t}\right] \tag{11}$$

The interaction is between the point projectile and a distributed density distribution in the nucleus, so the t^{-2} singularity in eq. (11) goes away and the (vt) distance may be replaced by r_o. Thus eq. (11) becomes

$$V(t) \simeq - \frac{2vR_t}{r_o^2} \exp\left[- \frac{(vt)^2}{2r_o R_t}\right] \tag{12}$$

Comparison of eqs. (2) and (12) indicates that the characteristic time t_o should be given by

$$t_o = \frac{\sqrt{2r_o R_t}}{v} \qquad (R_t >> r_o) \tag{13}$$

If the radius R_p of the projectile is comparable to that of the target R_t, then in eq. (13) one should replace R_t in the above equations by $R_t + R_p$.

A few words may be in order at this point. The latter value of t_o given by eq. (13) is 2-3 times bigger than the former value of r_o/v, the factor 2-3 arising from the size of the target nucleus. Longer interaction times have the effect of imparting a lower average excitation energy per excited nucleon of the target nucleus, as can be appreciated from the uncertainty principle. Hence, longer times of interaction would be in favor of inelastic excitation processes but against knock-out processes. It is not certain whether r_o should be the range of nucleon-nucleon interaction or the diffuseness parameter in a heavy ion optical potential.

Finally, the parameter L_o can be estimated to be equal to $2R_1/r_o$ in units of $\hbar$.

At low velocities the effective r_o for the nucleon-nucleon interaction may approach the pion-Compton wave length 1.4F characteristic for the attractive tail of the interaction. At higher velocities the effective r_o might approach the hard-core repulsive radius $\sim$ 0.4 F. The heavy-ion optical potentials have diffuseness parameters around 0.5 - 0.6 F.

3. Numerical Results

We apply our model to ${}^{208}_{82}Pb$, ${}^{88}_{38}Sr$ and ${}^{32}_{16}S$. For the nuclear radius R_t we use the relation $R_t = r_c A^{1/3}$ with $r_c = 1.24$ fm. For the effective nucleon-nucleon interaction range r_o we have chosen the value $r_o = 1.5$ fm. For the time-dependent Hamiltonian strength parameter V_1 we chose a strength that made the one-neutron removal product of yield unity. The angular momentum parameter L_o is evaluated from the relation $2R_1/r_o$ and is always rounded up to the closest integer. Our calculations have been done for three different values of t_o, one given by r_o/v, another by $\frac{r_o}{v}\sqrt{\frac{2R_t}{r_o}}$ and the third by $\frac{r_o}{v}\sqrt{\frac{2(R_t+R_p)}{r_o}}$. We have calculated the probabilities for various nuclear radii as well, and in one case for comparison we have introduced for L_o the value ∞, so that we eliminate any angular-momentum charge correction (suppression). Thus, Table I is calculated for a value of $ct_o = \frac{cr_o}{v}\sqrt{\frac{2R_t}{r_o}}$, Table II for $ct_o = \frac{cr_o}{v}$, and Table III is calculated for the same as I, ct_o and without the angular-momentum weighting factor ($L_o = \infty$). The velocity v of the projectile nucleus is for a kinetic energy of 250 MeV/nucleon. In all three tables inelastic scattering probabilities correspond to particle-hole excitations of protons or neutrons with residual energy less than a single neutron binding energy. Actually in our calculations we add to the neutron binding energy a few MeV since evaporation does not overtake gamma emission right at the neutron binding energy but higher[10]. The knock-out probabilities for either one neutron or one proton may consist of two parts. One is the clean knock-out which corresponds to a particle-continuum transition, and the other comes from the inelastic scattering followed by evaporation that is in our model particle-hole excitation with residual energy between two- and one-neutron binding energies and with the appropriate corrections to their numerical values as mentioned earlier. In the case of inelastic scattering followed by evaporation we have to calculate what fraction leads to neutron evaporation and what fraction to proton. To do so we assume an average excitation energy E^* given by

$$E^* = S_{1n} + \frac{S_{2n} - S_{1n}}{2} \tag{14}$$

with S_{1n} (S_{2n}) the one (two) neutron binding energy. From E^* we can calculate a corresponding nuclear temperature using the relation

$$E^* = 0.08\, A^{2/3}\, [Z^{1/3} + (A-Z)^{1/3}]\, (kT)^2 \tag{15}$$

Then the ratio of the probabilities of proton to neutron evaporation will be given by:

$$\frac{P(\text{proton evap.})}{P(\text{neutron evap.})} = \exp\left[-\frac{S_{1p} + V_c - S_{1n}}{kT}\right] \tag{16}$$

where in eq. (16) S_{1p} is one-proton binding energy and V_c is the Coulomb energy given by $V_c = \frac{Ze^2}{R}$ with R here equal to $r_c\, A^{1/3}$ and $r_c = 1.5$ fm. It turns out, as is expected, that only in the case of ^{32}S we have proton evaporation competing with neutron evaporation, but in the heavier nuclei, ^{88}Sr and ^{208}Pb, proton evaporation is virtually zero; that is, only neutron evaporation takes place in the case of ^{88}Sr and ^{208}Pb.

Another calculation which can be made with our model is that of finding the distribution of excitation probabilities versus spin for a given target nucleus. In these calculations we sort by total-angular momentum in the hole states and in the particle-hole states. The spatial delta interaction essentially results in a random two dimensional addition of the J vectors of particle and hole. More exactly for a given J_a and J_b, since only m = ± 1/2 states are involved and spin flip is not allowed, we have

$$P(I) = (\text{const}) \times (< J_a, J_b, 1/2, -1/2 \mid I, 0 >)^2 \tag{17}$$

In Fig. 1 such a distribution is plotted for ^{208}Pb.

4. Comparisons with Experiments and Monte Carlo Theory

Let us compare now for ^{208}Pb, ^{88}Sr, and ^{32}S relative knock-out cross sections for a neutron and a proton which includes clean knock-out (CKO) and inelastic scattering followed by one evaporation (ISE), and inelastic scattering (IS) cross sections. We can compare our results with i) Monte Carlo calculations done by K. Chen et al[10]), and ii) with the Bevalac experimental results of Ejiri et al[8]). Table IV provides such a comparison. Columns a,b have been obtained from ref. 10) and are the Monte Carlo calculations. Columns c,d,e are selected results from Tables I and II of our present calculation. Finally columns f,g are the experimental results of ref. 8). We have selected for columns c,d,e those results of Table I and II which seem the most reasonable in the light of both the Monte Carlo and the experimental results. The Monte Carlo results and our surface perturbation theory results seem to be rather close as far as the relative probabilities of inelastic scattering, inelastic scattering followed by one neutron (or proton) evaporation, and clean neutron or proton knock-out processes. Furthermore, the experimental results indicate larger probabilities for inelastic scattering than the knock-out processes of a proton or a neutron, contrary to the Monte Carlo and our surface perturbation calculation results. Another comparison which can be made between our calculation and existing experimental results is in the case of (p,pn) reactions the percentage of ISE and CKO neutrons. Yu et al[11]) have measured this percentage in ^{58}Ni and ^{97}Au, and Remsberg[12]) has measured it in ^{65}Cu with 400 MeV protons by recoil-products angular distribution measurements. Table V summarizes their results and includes the corresponding values of our calculation. It is immediately seen that our results agree at least qualitatively in that the CKO mechanism is dominant for light-mass targets whereas the ISE for heavy-mass targets becomes predominant. The agreement with our calculation is also fairly good, in fact far better than the Monte Carlo calculation. For comparison we include in the same table the pertinent Monte Carlo results. Note that the theoretical results of Table V have been transferred exactly from Table IV. Thus in our model calculation, we observe that the best agreement with both Monte Carlo and experimental results is obtained for the longer interaction distances corresponding to the target radius or target plus projectile radii for ^{88}Sr and ^{32}S. Furthermore, best agreement is obtained for an interaction time t_o less than that of eq. (3) for the approach of the nuclear surface and more nearly equal to the nucleon-nucleon collision time ($t_o = r_o/v$) for the nuclei ^{88}Sr and ^{32}S. It is apparent that our surface perturbation theory as well as the Monte Carlo calculation, both underestimate IS or ISE processes and tend to favor CKO ones. Insofar as our calculation is concerned, we would suggest that there may be a need to alter the nucleon-nucleon scattering differential cross sections away from their free space values. What is needed to enhance inelastic scattering to particle-hole states is increased small-angle scattering cross sections. In terms of effective force that is equivalent to increasing longer range components.

References

1. N. Metropolis et al, Phys. Rev. 110 (1958) 185; 110 (1958) 204
2. J. Hüfner et al, Phys. Rev. C 12 (1975) 1888
3. D. J. Lindstrom et al, LBL-3650 (1975) to be published
4. P. J. Karol and J. M. Miller, Phys. Rev. 166 (1968) 1089
5. P. A. Benioff, Phys. Rev. 119 (1960) 324
6. N. Marty et al, Nucl. Phys. A238 (1975) 93
7. R. Bertini et al, Phys. Letters 45B (1973) 119
8. H. Ejiri et al, LBL-4398 (1976) to be published
9. V. G. Soloviev, Theory of Complex Nuclei, Pergamon N.Y., (1975) p. 21
10. K. Chen et al, Phys. Rev. 166 (1968) 949
11. Y.-W. Yu et al, Nucl. Phys. A152 (1970) 295
12. L. P. Remsberg, Phys. Rev. 174 (1968) 1338

Figure Captions

Fig. 1 Distribution of excitation probabilities versus target-spin.

(a) IS; (b) CKO; (c) ISE .

TABLE I*

Relative Contributions of IS, ISE, CKO Processes for Interaction Time $t_o = \frac{r_o}{v}\sqrt{\frac{2R_1}{r_o}}$

Target Nucleus		$^{208}_{82}Pb$		$^{32}_{16}S$			$^{88}_{38}Sr$	
Nuclear Radius $R_o = r_c A^{1/3}$ & Interaction Time $t_o c$ (fm)		R_o=7.35,	$t_o c$=7.61	R_o=4.00	$t_o c$=5.61		R_o=5.53,	$t_o c$=6.60
Interaction Distance R_1 (fm)		7.30	8.30	3.50	4.00	5.00	5.50	6.50
Inelastic Scattering (IS) (p&n)	$E^* \leq S_{1n}$	0.72	0.384	1.615	1.405	0.547	0.686	0.337
	ISE $S_{1n} \leq E^* \leq S_{2n}$	0.4368	0.151	0.330	0.150	0.034	0.473	0.170
Knock-out neutron	CKO	0.5632	0.849	0.770	0.850	0.966	0.577	0.830
	Total	1.0000	1.000	1.000	1.000	1.000	1.000	1.000
	ISE $S_{1n} \leq E^* \leq S_{2n}$	0.0000	0.0000	0.349	0.234	0.0530	0.000	0.000
Knock-out neutron	CKO	0.1763	0.1400	0.777	0.857	0.882	0.281	0.338
	Total	0.1763	0.1400	1.126	0.090	0.935	0.281	0.338

*Results are normalized so that neutron knock-out total 1.000

TABLE II*

Relative contributions of IS, ISE, CKO processes for $t_o = r_o/v$

Target Nucleus Nuclear Radius $R_o = r_c A^{1/3}$ & Interaction Time $t_o c$ (fm)	$^{208}_{82}Pb$ $R_o = 7.35$, $t_o c = 2.43$		$^{32}_{16}S$ $R_o = 4.00$ $t_o c = 2.43$			$^{88}_{38}Sr$ $R_o = 5.53$ $t_o c = 2.43$	
Interaction Distance R_1 (fm)	7.30	8.30	3.50	4.00	5.00	5.50	6.50
Inelastic Scattering (IS) (p & n) $E^* \leq S_{1n}$	0.274	0.126	0.663	0.687	0.273	0.353	0.153
1-neutron removal: ISE $S_{1n} \leq E^* \leq S_{2n}$	0.189	0.057	0.125	0.079	0.020	0.274	0.086
1-neutron removal: Total	1.0000	1.0000	1.000	1.000	1.000	1.000	1.000
1-neutron removal: CKO	0.811	0.943	0.875	0.921	0.980	0.726	0.914
1-proton removal: ISE $S_{1n} \leq E^* \leq S_{2n}$	0.000	0.000	0.199	0.126	0.031	0.000	0.000
1-proton removal: Total	0.352	0.228	0.979	0.976	0.936	0.418	0.415
1-proton removal: CKO	0.352	0.228	0.780	0.850	0.905	0.418	0.415

*Results are normalized so that neutron knock-out totals 1.000

TABLE III*

Relative Contributions of IS, ISE, CKO Without Inclusion of Angular-momentum Transfer Suppression Factor

Target Nucleus		$^{208}_{82}Pb$	
Nuclear Radius $R_o = r_c A^{1/3}$ & Interaction time $t_o c$ (fm)		$R_o = 7.35$	$ct_o = 7.61$
Distance R_1 (fm)		7.30	8.30
Inelastic Scattering (IS) (p&n)	$E^* \leq S_{1n}$	0.289	0.142
Knock-Out neutron	ISE $S_{1n} \leq E^* \leq S_{2n}$	0.175	0.056
	Total	1.000	1.000
	CKO	0.825	0.994
Knock-Out proton	ISE $S_{1n} \leq E^* \leq S_{2n}$	0.000	0.000
	Total	0.249	0.139
	CKO	0.249	0.139

*Results normalized so that neutron Knock-out totals 1.000. Angular-momentum parameter $L_o = \infty$

TABLE IV

Comparison of Monte Carlo Calculation, present work, and experiment

Target Nucleus		^{75}As (a)	^{209}Bi (b)	^{32}S (c) $ct_o=2.43$	^{88}Sr (d) $ct_o=2.43$	^{208}Pb (e) $ct_o=7.61$	^{23}Na (f)	^{40}Ca (g)
Inelastic Scattering (IS)		0.234	0.200	0.687	0.353	0.720	1.42±0.20	2.87±1.02
Knock-out neutron	ISE	0.303	0.314	0.079	0.274	0.437		
	Total	1.000	1.000	1.000	1.000	1.000	1.00±0.221	1.00±0.47
	CKO	0697	0.686	0.921	0.726	0.563		
Knock-out proton	ISE	0.000	0.000	0.126	0.000	0.000		
	Total	0.586	0.476	0.976	0.418	0.176	1.64±0.39	1.80±0.53
	CKO	0.586	0.476	0.850	0.418	0.176		

a-b: Monte Carlo calculations taken from K. Chen et al[10] and appropriately normalized a: 378 MeV P on ^{75}As; b: 375 MeV p on $^{209}B_i$; (STEPNO code for both cases)

c-e: Present calculation 256 MeV/N. Results selected from Tables I and II

f-g: Experimental results of H. Ejiri et al[8]. 400 MeV/N ^{12}C on ^{40}Ca and ^{23}Na.

TABLE V

Relative Contributions of ISE and CKO processes for (p&n) reactions

Energy of projectile (Source of information)	400 MeV p, Y.-w Yu *et al*[11] Exp. Results		400 MeV p, Remsberg[12] Exp. Results	Present Calculation 256 MeV/Nucleon (Parameters for each case appear below)			378 MeV p on ^{75}As, 375 MeV p on ^{209}Bi, Monte Carlo calculation by K. Chen *et al*[10]	
Target	^{197}Au	^{58}Ni	^{65}Cu	^{208}Pb	^{88}Sr	^{32}S	^{209}Bi	^{75}As
Knock-out neutron: ISE	0.55	0.05	0.28	0.44	0.27	0.08	0.314	0.303
Knock-out neutron: CKO	0.45	0.95	0.72	0.56	0.73	0.92	0.686	0.657
				R_o=7.35	R_o=5.53	R_o=4.00		
				R_{int}=7.3	R_{int}=5.50	R_{int}=4.00		
				t_oc=7.61	t_oc=2.43	t_oc=2.43		
				(in fm)				

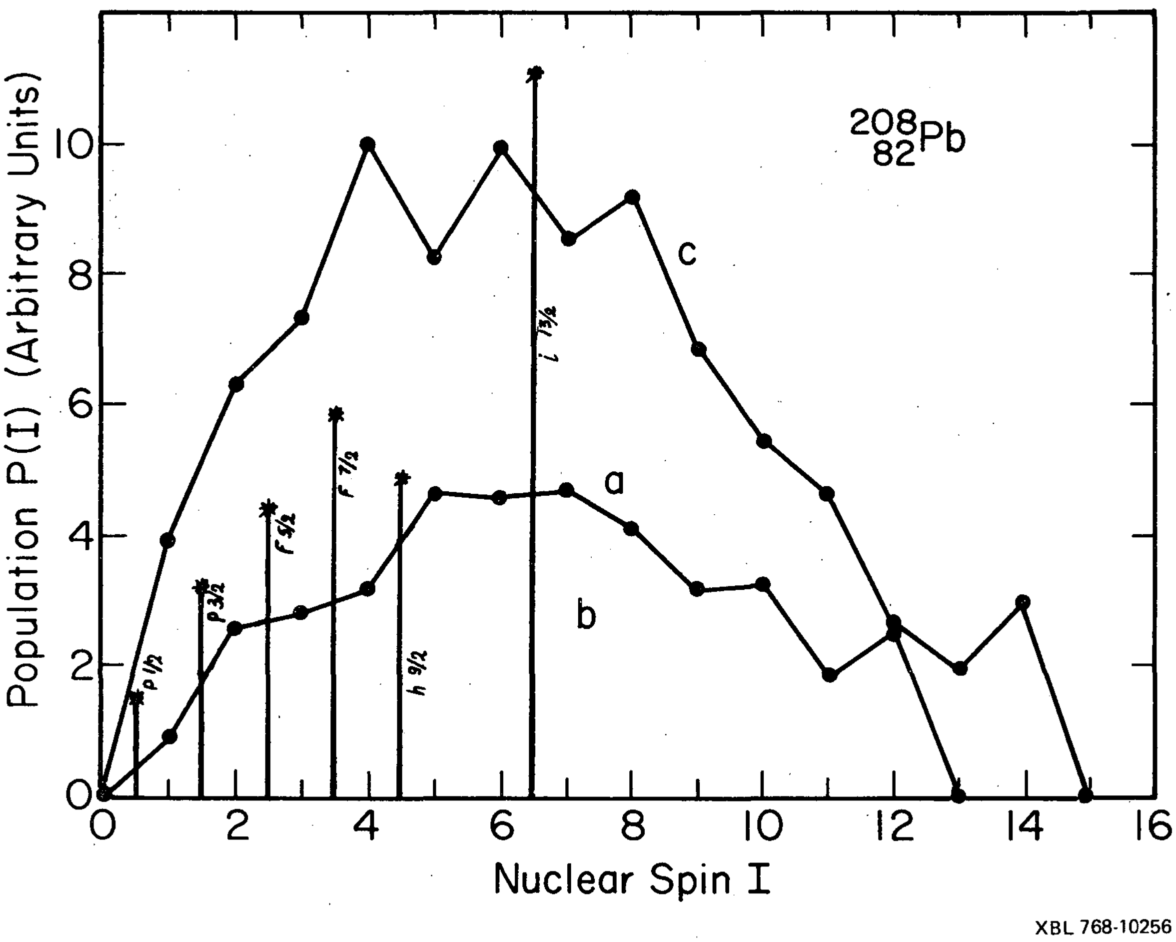

Population P(I) (Arbitrary Units)
Nuclear Spin I
$^{208}_{82}Pb$
a
b
c
p 1/2
p 3/2
f 5/2
f 7/2
h 9/2
i 13/2
0
2
4
6
8
10
12
14
16
XBL 768-10256

Fig. 1

TECHNICAL INFORMATION DIVISION
LAWRENCE BERKELEY LABORATORY
UNIVERSITY OF CALIFORNIA
BERKELEY, CALIFORNIA 94720